Available online at www.sciencedirect.com
ScienceDirect
Journal of Catalysis 255 (2008) 213–219
JOURNAL OF CATALYSIS
www.elsevier.com/locate/jcat

Transformation of nano-sized vanadyl hydrogen phosphate hemihydrate crystallites to vanadyl pyrophosphate during activation in the presence of *n*-butane and oxygen

Hiroyuki Imai, Yuichi Kamiya *, Toshio Okuhara

Research Faculty of Environmental Earth Science, Hokkaido University, Sapporo 060-0810, Japan

Received 19 December 2007; revised 5 February 2008; accepted 7 February 2008

Available online 10 March 2008

Abstract

The transformation of nano-sized $VOHPO_4{\cdot}0.5H_2O$ crystallites (340 nm × 40 nm) to $(VO)_2P_2O_7$ was examined. The crystalline structure of $VOHPO_4{\cdot}0.5H_2O$ quickly collapsed to form an oxidized amorphous phase within 1 h (reaction conditions: 1.5% *n*-butane, 17% O_2, and 81.5% He at 663 K), followed by gradual crystallization to $(VO)_2P_2O_7$, accompanied by the formation of sharply angular nano-sized crystallites (about 50 nm). No crystalline phases other than $(VO)_2P_2O_7$ were formed during this transformation. This is quite different from the transformation of large and thick $VOHPO_4{\cdot}0.5H_2O$ crystallites, in which α_{II}-$VOPO_4$ and δ-$VOPO_4$ have been detected in the resulting catalyst. The selectivity to maleic anhydride increases during the transformation as a result of the formation of $(VO)_2P_2O_7$. The activity increases in the early stages of the transformation, then decreases with time. The decrease in activity is caused by gradual reduction of the catalyst surface during the transformation.

Keywords: *n*-Butane oxidation; Vanadyl pyrophosphate; Nano-crystallites; Transformation; Microstructure

1. Introduction

Vanadyl pyrophosphate, $(VO)_2P_2O_7$, is a major active component of a catalyst used for selective oxidation of *n*-butane to maleic anhydride (MA) [1–3]. The $(VO)_2P_2O_7$ catalyst is derived from the precursor $VOHPO_4{\cdot}0.5H_2O$ by thermal treatment under an inert atmosphere. An active and selective catalyst also has been produced by treating $VOHPO_4{\cdot}0.5H_2O$ in an *n*-butane/air mixture at 600–750 K for more than 100 h [1,2,4,5].

Under these reaction conditions, the transformation from $VOHPO_4{\cdot}0.5H_2O$ to $(VO)_2P_2O_7$ proceeds through a complicated process involving dehydration, oxidation, and reduction [6–10]. Because the microstructure of the solid sample changes with treatment time, so do the selectivity and activity in *n*-butane oxidation. Thus, investigation of the transformation provides valuable information on factors influencing the selectivity and activity of the $(VO)_2P_2O_7$ catalyst.

Abon et al. [6] proposed that in the initial stage, $VOHPO_4{\cdot}0.5H_2O$ is in part transformed into $(VO)_2P_2O_7$ through topotactic transformation and in part oxidized to δ-$VOPO_4$, which is then reduced to $(VO)_2P_2O_7$ in the reaction gas (n-$C_4H_{10}/O_2/He = 1.6/18/80.4$) at 673 K, becoming completely reduced after a long time on stream. They also suggested that the V^{4+}/V^{5+} ratio on the surface of the catalyst is an important factor in controlling the activity; that is, a catalyst with a high V^{4+}/V^{5+} ratio exhibits high activity. Hutchings et al. [7] observed the transformation through in-situ laser Raman spectroscopy; as temperature was increased from room temperature to 667 K, the peaks due to $VOHPO_4{\cdot}0.5H_2O$ completely disappeared at 643 K, and peaks attributed to $(VO)_2P_2O_7$ as well as α_{II}-, γ-, and δ-$VOPO_4$ appeared instead, until only a strong peak for $(VO)_2P_2O_7$ was observed at 667 K. O'Mahony et al. [10] reported that during the activation process in *n*-butane/air mixture, $(VO)_2P_2O_7$ was formed at 573 K with no intermediate amorphous phase. Conte et al. [11], using in-situ XRD, observed the formation of ε-$VOPO_4$ from $VOHPO_4{\cdot}0.5H_2O$ in N_2 and its rapid transformation into δ-$VOPO_4$ through exposure to *n*-butane at the reaction temperature.

* Corresponding author. Fax: +81 11 706 4513.
E-mail address: kamiya@ees.hokudai.ac.jp (Y. Kamiya).

0021-9517/$ – see front matter
doi:10.1016/j.jcat.2008.02.002

Kiely et al. [8] observed the formation of catalysts containing $(VO)_2P_2O_7$ and crystalline $VOPO_4$ (V^{5+}) phases in certain proportions from precursors prepared by different preparation methods. These results prompted an investigation of the effect of $VOHPO_4{\cdot}0.5H_2O$ crystallite size on the crystalline phase and microstructure of the resulting catalysts. The data clearly demonstrated that micrometer-sized crystallites (1000 nm × 110 nm) of $VOHPO_4{\cdot}0.5H_2O$ transformed into a single phase of $(VO)_2P_2O_7$, whereas large crystallites (10,000 nm × 415 nm) transformed into catalyst particles consisting of peripheral $(VO)_2P_2O_7$ and internal α_{II}-$VOPO_4$ under reaction conditions of 1.5% *n*-butane, 17% O_2, and 81.5% He at 663 K for 300 h [12]. The catalyst derived from micrometer-sized $VOHPO_4{\cdot}0.5H_2O$ crystallites showed relatively high activity and selectivity for the oxidation of *n*-butane compared with those from the large crystallites.

Much smaller and thinner $VOHPO_4{\cdot}0.5H_2O$ crystallites (340 nm × 40 nm) have been successfully synthesized by exfoliation–reduction of $VOPO_4{\cdot}2H_2O$ in a mixture of 2-butanol/ethanol [13,14]. The $(VO)_2P_2O_7$ catalyst derived from nano-sized $VOHPO_4{\cdot}0.5H_2O$ crystallites exhibited extremely high selectivity to MA (about 84% at 47% conversion and 78% even at 85% conversion at 663 K). Interestingly, in contrast to micrometer-sized $VOHPO_4{\cdot}0.5H_2O$, the resulting catalyst was composed of crystallites about 50 nm in length, much smaller than those of the starting $VOHPO_4{\cdot}0.5H_2O$ crystallites (340 nm long).

The present study examined changes in the microstructure of solid samples during transformation of nano-sized $VOHPO_4{\cdot}0.5H_2O$ crystallites to $(VO)_2P_2O_7$ using X-ray diffraction (XRD), Raman spectroscopy, X-ray photoelectron spectroscopy (XPS), redox titration, N_2 adsorption–desorption isotherms, scanning electron microscopy (SEM), and temperature-programmed reduction (TPR). Furthermore, changes in the activity and selectivity for *n*-butane oxidation during the transformation in relation to the physicochemical properties of the catalyst (including microstructure and redox properties) were evaluated, to provide insight into factors affecting the catalyst activity and selectivity during the oxidation of *n*-butane.

2. Experimental

2.1. Preparation of nano-sized $VOHPO_4{\cdot}0.5H_2O$ crystallites

$VOPO_4{\cdot}2H_2O$, which served as the raw material for nano-sized $VOHPO_4{\cdot}0.5H_2O$ crystallites, was prepared as follows. A mixture of V_2O_5 (24 g, Wako Pure Chem. Ind., Ltd.), aqueous 85% H_3PO_4 (223 g, Wako Pure Chem. Ind., Ltd.), and H_2O (577 cm^3) was refluxed for 16 h. The resulting precipitate was separated by filtration, washed with acetone, and dried under ambient atmosphere. The resulting yellow solid was identified as $VOPO_4{\cdot}2H_2O$ by XRD and IR [15].

Nano-sized $VOHPO_4{\cdot}0.5H_2O$ crystallites were prepared by exfoliation–reduction of $VOPO_4{\cdot}2H_2O$ in a mixture of 2-butanol and ethanol, as reported previously [13]. A mixture of $VOPO_4{\cdot}2H_2O$ (1.0 g) and 2-butanol (50 cm^3, Wako Pure Chem. Ind., Ltd.) was heated stepwise at 303, 323, 343, and 363 K for 1 h at each temperature under stirring to form a homogeneous solution containing exfoliated $VOPO_4$ sheets as the product of intercalation, followed by exfoliation of $VOPO_4{\cdot}2H_2O$ [16]. To the resulting homogeneous 2-butanol solution, ethanol (14.4 cm^3, Wako Pure Chem. Ind., Ltd.) was added at room temperature, and then this solution was refluxed for 20 h (reduction) to form a light-blue precipitate. This precipitate was separated by centrifugation, washed with acetone, and dried at room temperature overnight to obtain nano-sized $VOHPO_4{\cdot}0.5H_2O$ crystallites.

2.2. Transformation of nano-sized $VOHPO_4{\cdot}0.5H_2O$ into catalyst

Transformation of nano-sized $VOHPO_4{\cdot}0.5H_2O$ to the catalyst was performed at 663 K in a flow reactor (Pyrex tube, 10 mm i.d.) under atmospheric pressure. After $VOHPO_4{\cdot}0.5H_2O$ powder (0.20 g) was placed in the reactor, reactant gas consisting of 1.5% *n*-butane, 17% O_2, and 81.5% He was added at a flow rate of 10 $cm^3\,min^{-1}$. The temperature was raised from room temperature to 663 K at a rate of 5 $K\,min^{-1}$ and then maintained at 663 K. To observe structural changes of the solids during the transformation, solid samples were prepared under different treatment times (1, 5, 10, 15, 31, 120, and 300 h after the temperature reached 663 K). After the predetermined time, the reactor was cooled rapidly to room temperature. The samples were stored in vacuo until characterized. A sample treated for x h is designated $S_{x\mathrm{h}}$.

During the transformation, the gas at the outlet of the reactor was analyzed by online gas chromatography. A Shimadzu GC-8A gas chromatograph equipped with flame ionization detector and a Porapak QS column (1 m) was used to analyze *n*-butane and MA; an Area M200 high-speed gas chromatograph with Porapak Q and molecular sieve 5A columns was used to analyze CO, CO_2, and O_2.

2.3. Characterization

The powder XRD patterns of the solid samples were measured with a Rigaku Miniflex XRD diffractometer with CuK_α radiation. Raman spectra of the solid samples were obtained with a JASCO RMP-230 Raman spectrometer. Adsorption–desorption isotherms of nitrogen were obtained at 77 K with a BEL Japan Belsorp 28SA automatic adsorption apparatus after evacuation of the chamber containing the sample at 423 K for 1 h. Specific surface area was calculated using the BET method.

SEM images were obtained with a Hitachi FE-SEM S-4800 instrument. The average oxidation number of V in the sample bulk was determined using a redox-titration method with $KMnO_4$ [17]. XPS was carried out on a Shimadzu XPS-7000 instrument with MgK_α radiation. The average oxidation number of V on the surface was estimated as described previously [6].

TPR profiles were obtained using a custom apparatus equipped with an Anelva M-200Q quadrupole mass spectrometer. A sample of approximately 0.02 g was fixed in a quartz U-shaped tube and pretreated under He flow (20 $cm^3\,min^{-1}$) at

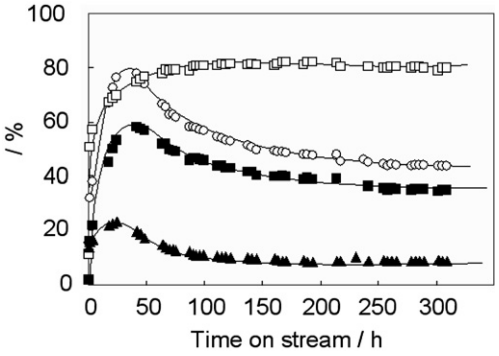

Fig. 1. Time course changes for selective oxidation of *n*-butane during transformation of nano-sized $VOHPO_4{\cdot}0.5H_2O$. The reaction was conducted at 663 K in a mixture of 1.5% *n*-butane, 17% O_2, and 81.5% He. (○) Conversion of *n*-butane; (□) selectivity to MA; (■) yield of MA; (▲) yield of CO_x.

423 K for 1 h. After the pretreatment, the gas was switched to H_2 and the temperature increased at a rate of 10 K min^{-1} while monitoring signals of $m/e = 18$.

3. Results

Fig. 1 shows the time course for the selective oxidation of *n*-butane at 663 K. The conversion of *n*-butane was low initially (0 h), then increased rapidly up to 30–40 h. After reaching maximum conversion, the level of conversion decreased gradually, until a constant value was achieved at 300 h. Selectivity to MA was very low at the beginning of the reaction but increased dramatically to 75% within the first 40 h, finally reaching a constant value of 82% after 100 h. As a result, the yield of MA showed a trend similar to that of the conversion rate.

Fig. 2 shows changes in the XRD patterns of the samples during transformation from the precursor $VOHPO_4{\cdot}0.5H_2O$ to the catalyst, as well as changes in the intensities of diffraction lines attributed to the (200), (042), and (023) planes. The precursor was confirmed to be crystalline $VOHPO_4{\cdot}0.5H_2O$. The intense diffraction lines attributed to $VOHPO_4{\cdot}0.5H_2O$ disappeared completely, and no diffraction line was observed at 1 h, indicating the amorphous nature of S_{1h}. At 5 h, very weak diffraction lines attributed to the $(VO)_2P_2O_7$ phase appeared. The intensities of the diffraction lines due to $(VO)_2P_2O_7$ increased rapidly up to 31 h and more slowly thereafter (Fig. 2B). After 300 h, only the XRD pattern attributed to the highly crystalline $(VO)_2P_2O_7$ was observed.

Fig. 3 shows changes in the Raman spectra of the samples during the transformation. These changes are consistent with those seen in the XRD patterns. Only peaks attributed to $VOHPO_4{\cdot}0.5H_2O$ (985, 1106, and 1150 cm^{-1}) were observed for the precursor. These peaks disappeared completely at 1 h, and no peaks were observed until 10 h. A peak assigned to $(VO)_2P_2O_7$ appeared at 926 cm^{-1} after 15 h and increased in intensity.

Fig. 4 shows SEM images of the precursor and samples treated over different durations. The precursor was composed of small, thin, leaf-like crystallites with an average lateral length of 300 nm. The thickness was estimated as 40 nm from the SEM images. The shape and size of the sample crystallites were similar to those of the precursor up to 10 h; however, at 15 h, many cracks appeared on the crystallites, and very small crystallites with a rectangular shape began to appear. Finally, at 300 h, these crystallites were completely transformed into angular, nanosized crystallites of approximately 50 nm on the narrow side and 100 nm on the long side.

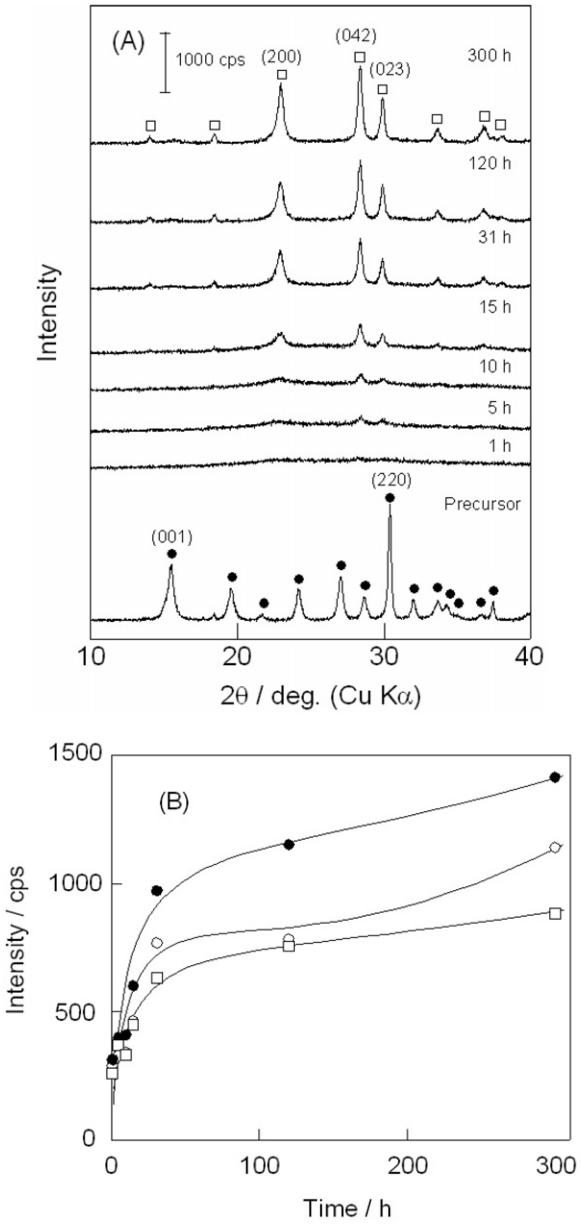

Fig. 2. Changes in: (A) XRD patterns of the samples during the transformation [● and □ represent $VOHPO_4{\cdot}0.5H_2O$ and $(VO)_2P_2O_7$, respectively]; (B) intensity of diffraction lines as a function of treatment time [(○) (200) plane; (●) (042) plane; (□) (023) plane]. The transformation was conducted at 663 K in a mixture of 1.5% *n*-butane, 17% O_2, and 81.5% He.

Fig. 5 shows changes in surface area (Fig. 5A) and oxidation number of V on the surface and in the bulk (Fig. 5B) as a function of treatment time (with values at 0 h representing those of the precursor). The precursor had a surface area of 23 $m^2\ g^{-1}$, which increased nearly twofold after treatment for 300 h, reaching a value of 39 $m^2\ g^{-1}$. As shown in Fig. 5B, the V oxidation

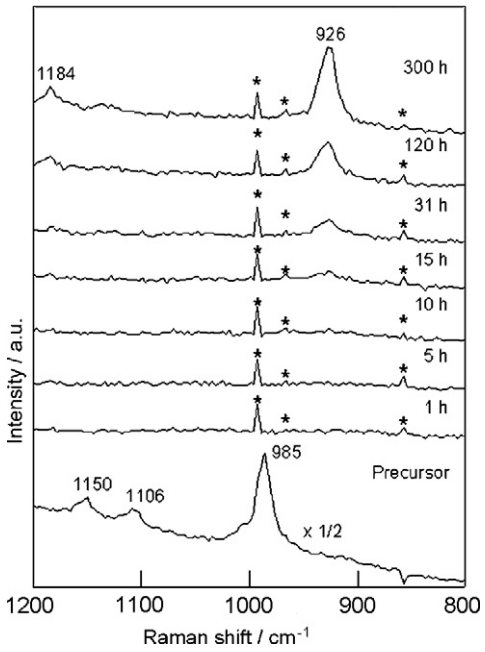

Fig. 3. Changes in Raman spectra of samples during the transformation from the precursor to the catalyst. The transformation was conducted at 663 K in a mixture of 1.5% *n*-butane, 17% O_2, and 81.5% He.

number increased dramatically to a maximum after 1 h ($V^{4.78+}$ for the surface and $V^{4.40+}$ for the bulk). The oxidation numbers then gradually decreased and become constant at 300 h ($V^{4.18+}$ for the surface and $V^{4.06+}$ for the bulk). The surface was more highly oxidized at 31 h than at 300 h, whereas the oxidation state of the sample bulk was nearly the same at 31 h as at 300 h. To further investigate this difference, we measured TPR profiles of the samples at 31 and 300 h (Fig. 6). In the spectra, the peaks at 780 and 920 K are assignable to the reduction of V^{5+} and V^{4+}, respectively. As shown in Fig. 6, the V^{5+} peak was observed for S_{31h}. In contrast, the peak at 780 K was absent for S_{300h}, clearly indicating that the sample was more highly oxidized at 31 h than at 300 h.

4. Discussion

Previous studies have reported on the transformation of $VOHPO_4{\cdot}0.5H_2O$, which tends to have relatively large crystallites, to an active catalyst form [6–12]. The present study investigated the transformation of nano-sized $VOHPO_4{\cdot}0.5H_2O$ crystallites (300 nm long, 40 nm thick). The resulting catalyst showed excellent selectivity to MA, as was described previously [13,14].

Whereas the nano-sized precursor $VOHPO_4{\cdot}0.5H_2O$ was highly crystalline, its crystal structure quickly collapsed into an amorphous phase just after the start of treatment (1 h; Figs. 2A and 3), accompanied by deep oxidation of the surface and bulk. This finding indicates that the surface and bulk of the crystallites were both oxidized during the initial stage of transformation, whereas any change in morphology during this process ($VOHPO_4{\cdot}0.5H_2O \rightarrow$ partially oxidized amorphous) was small and any change in surface area was negligible. In terms of catalytic properties for the amorphous material, S_{5h} and S_{10h} exhibited decent activity and selectivity to MA (Fig. 1), whereas they were basically amorphous. Because the amorphous phase was formed simply by the dehydration and partial oxidation of $VOHPO_4{\cdot}0.5H_2O$, we can assume that crystallographic regularity of $VOHPO_4{\cdot}0.5H_2O$, such as V–O–V dimer structure,

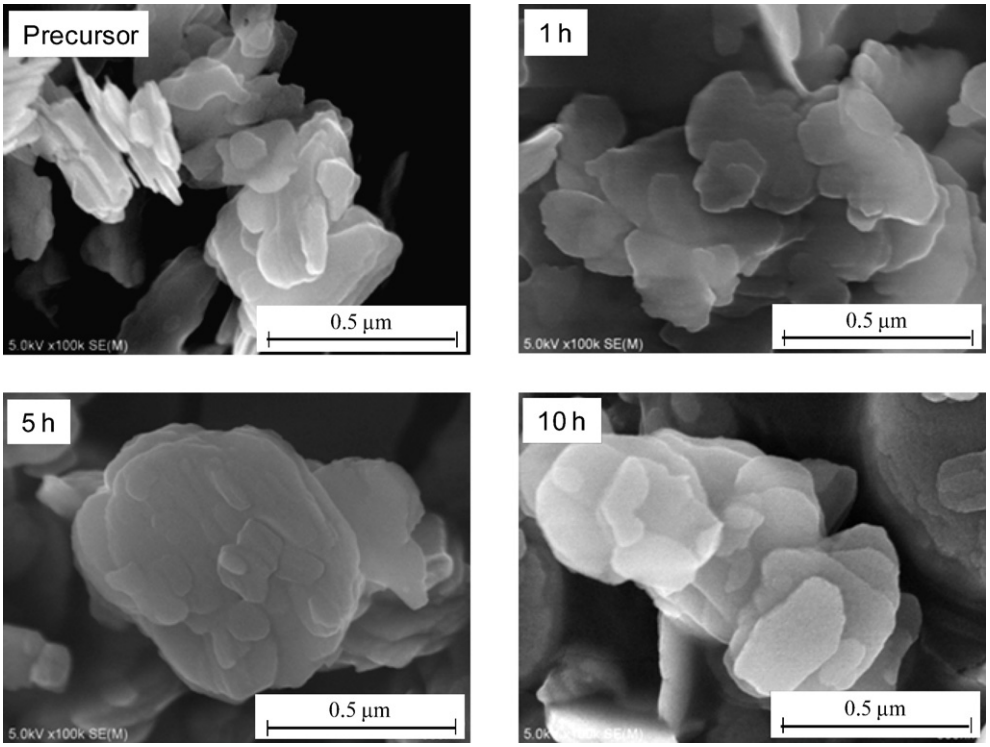

Fig. 4. SEM images of samples at different times. The transformation was conducted at 663 K in a mixture of 1.5% *n*-butane, 17% O_2, and 81.5% He.

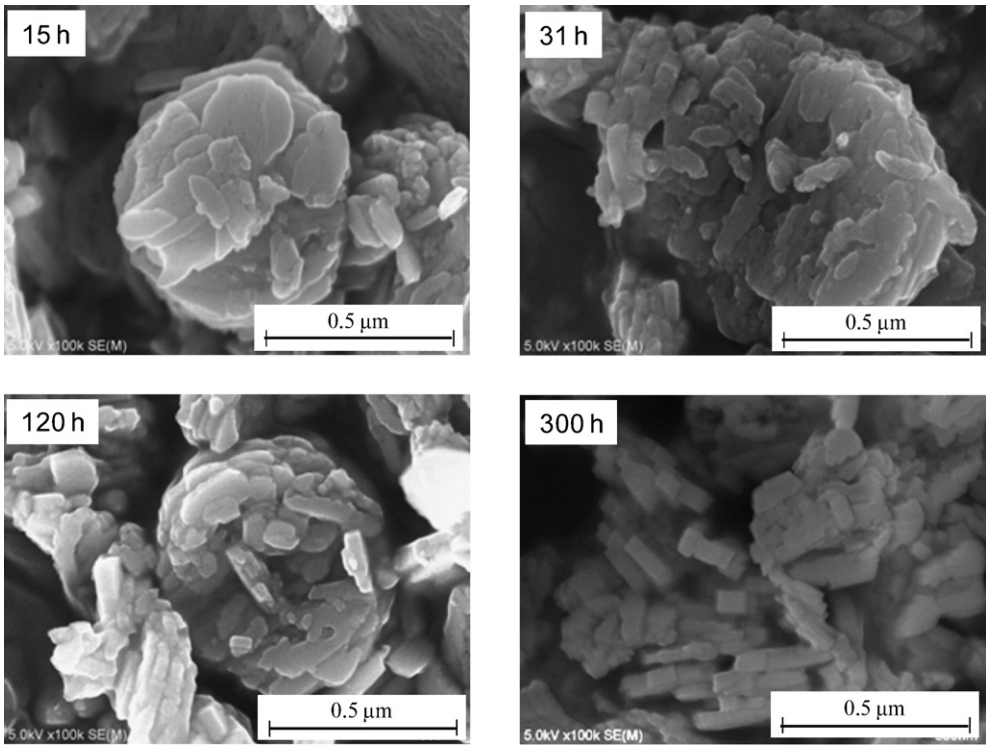

Fig. 4. (*continued*)

remained partly in the amorphous phase. This may have led to the decent activity and selectivity for these amorphous materials. Hutchings et al. [18,19] reported that an amorphous VPO material (VPO_{LP}) prepared using liquid CO_2 partially crystallized under the reaction conditions of the *n*-butane oxidation, but another amorphous VPO (VPO_{SCP}) synthesized in supercritical CO_2 did not crystallize even under the such conditions over a long period. Because our amorphous material was gradually transformed into crystalline $(VO)_2P_2O_7$ under the reaction conditions, it may have a similar structural nature to the VPO_{LP}.

Crystalline phases other than $(VO)_2P_2O_7$ were not observed by XRD (Fig. 2A) or Raman spectroscopy (Fig. 3) for samples obtained during transformation from the partially oxidized amorphous (S_{1h}) to $(VO)_2P_2O_7$ (S_{300h}). These results suggest that the nano-sized $VOHPO_4{\cdot}0.5H_2O$ crystallites could transform to crystalline $(VO)_2P_2O_7$ as follows: $VOHPO_4{\cdot}0.5H_2O$ → partially oxidized amorphous phase → highly crystalline $(VO)_2P_2O_7$.

The SEM images (Fig. 4) show the formation of much smaller crystallites after the appearance of cracks on the crystallites at 15 h. These smaller crystallites steadily transform into much smaller nano-sized rectangular crystallites with increasing treatment time. Because the formation of these rectangular crystallites was coincident with the appearance of the $(VO)_2P_2O_7$ phase in the XRD and Raman spectra, the rectangular crystallites observed in S_{15h} were $(VO)_2P_2O_7$ crystallites. As reported previously [13], TEM and selected-area electron diffraction (ED) of S_{300h} demonstrated that the rectangular nano-sized crystallites of S_{300h} consisted of single crystals of $(VO)_2P_2O_7$. At the onset of crystallization of $(VO)_2P_2O_7$ (S_{15h}), an amorphous phase remains, as shown by the very

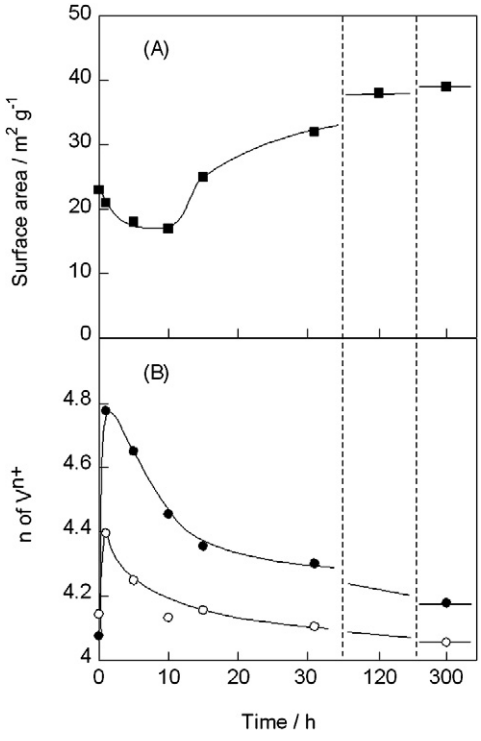

Fig. 5. Changes in (A) surface area and (B) average oxidation number of V [(●) on the surface and (○) in bulk] as a function of treatment time. The transformation was conducted at 663 K in a mixture of 1.5% *n*-butane, 17% O_2, and 81.5% He.

broad line at around 20–25° of 2θ in Fig. 2A. The morphological heterogeneity observed in the SEM image of S_{15h} supports this result. These findings suggest that $(VO)_2P_2O_7$ was partially formed in the crystallite, leading to the smaller crystallites.

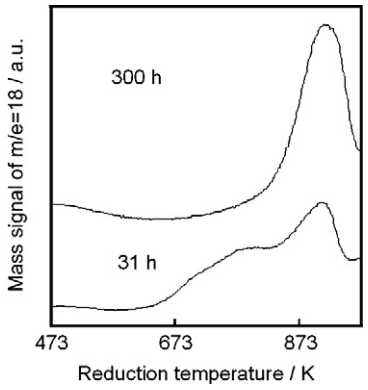

Fig. 6. Temperature-programmed reduction profiles for samples treated for 31 and 300 h at 663 K.

The surface area increased considerably after 15 h (Fig. 5A) due to morphological changes in the solid caused by formation of crystalline $(VO)_2P_2O_7$. Schematic models of the crystallites during transformation of nano-sized $VOHPO_4{\cdot}0.5H_2O$ to $(VO)_2P_2O_7$ are depicted in Fig. 7.

The striking difference between the results of the present study and those of previous studies of the transformation of $VOHPO_4{\cdot}0.5H_2O$ is the observation of crystalline phases formed during the intermediate stages of transformation. No crystalline phases were formed from nano-sized $VOHPO_4{\cdot}0.5H_2O$, whereas $VOPO_4$ phases, including α_{II}-$VOPO_4$ and δ-$VOPO_4$, are known to be temporarily formed from larger $VOHPO_4{\cdot}0.5H_2O$ crystallites [6–9,12]. Using TEM, XRD, and ^{31}P NMR spin-echo mapping, Kiely et al. [9] demonstrated that the transformation from $VOHPO_4{\cdot}0.5H_2O$ (2 μm long, 100 nm thick) to $(VO)_2P_2O_7$ proceeds via formation of δ-$VOPO_4$ as an intermediate, followed by reduction to $(VO)_2P_2O_7$, in the interior of the crystallites, whereas the $(VO)_2P_2O_7$ phase is formed directly on simple dehydration of $VOHPO_4{\cdot}0.5H_2O$ (topotactic transformation) at the periphery of the crystallites. Similarly, Abon et al. [6] demonstrated that $VOHPO_4{\cdot}0.5H_2O$ is partially transformed into $(VO)_2P_2O_7$ through topotactic transformation and partially into $(VO)_2P_2O_7$ via the δ-$VOPO_4$ phase. Kamiya et al. [12] reported that crystallite size affects the transformation and that the subsequent microstructure and phases of the resulting catalysts depend on the size of the $VOHPO_4{\cdot}0.5H_2O$ crystallites. The micrometer-sized $VOHPO_4{\cdot}0.5H_2O$ crystallites (1000 nm × 110 nm) transform into a single phase $(VO)_2P_2O_7$ with a high specific surface area, whereas the catalyst derived from the large $VOHPO_4{\cdot}0.5H_2O$ crystallites (10,000 nm × 415 nm) comprises particles with a double-layer structure, consisting of peripheral $(VO)_2P_2O_7$ and internal α_{II}-$VOPO_4$.

In those previous studies, the catalyst particles contained a double-layer structure, comprising peripheral $(VO)_2P_2O_7$ crystallites and internal crystallites including $(VO)_2P_2O_7$, δ-$VOPO_4$, or α_{II}-$VOPO_4$, whereas the apparent shape and size (morphology) of the catalyst particles were very similar to those of the starting $VOHPO_4{\cdot}0.5H_2O$. In contrast, the nano-sized $VOHPO_4{\cdot}0.5H_2O$ (300 nm long, 40 nm thick) crystallites observed in the present work, which were much smaller than those reported previously, transformed into a bare, single crystal of $(VO)_2P_2O_7$ that did not have a double-layer structure. During the transformation from $VOHPO_4{\cdot}0.5H_2O$ to $(VO)_2P_2O_7$, dehydration of crystalline water is inevitable regardless of the treatment conditions (reactant gas or inert gas). For large $VOHPO_4{\cdot}0.5H_2O$ crystallites, water at the periphery of the crystallites likely can readily escape, leading to topotactic transformation from $VOHPO_4{\cdot}0.5H_2O$ to

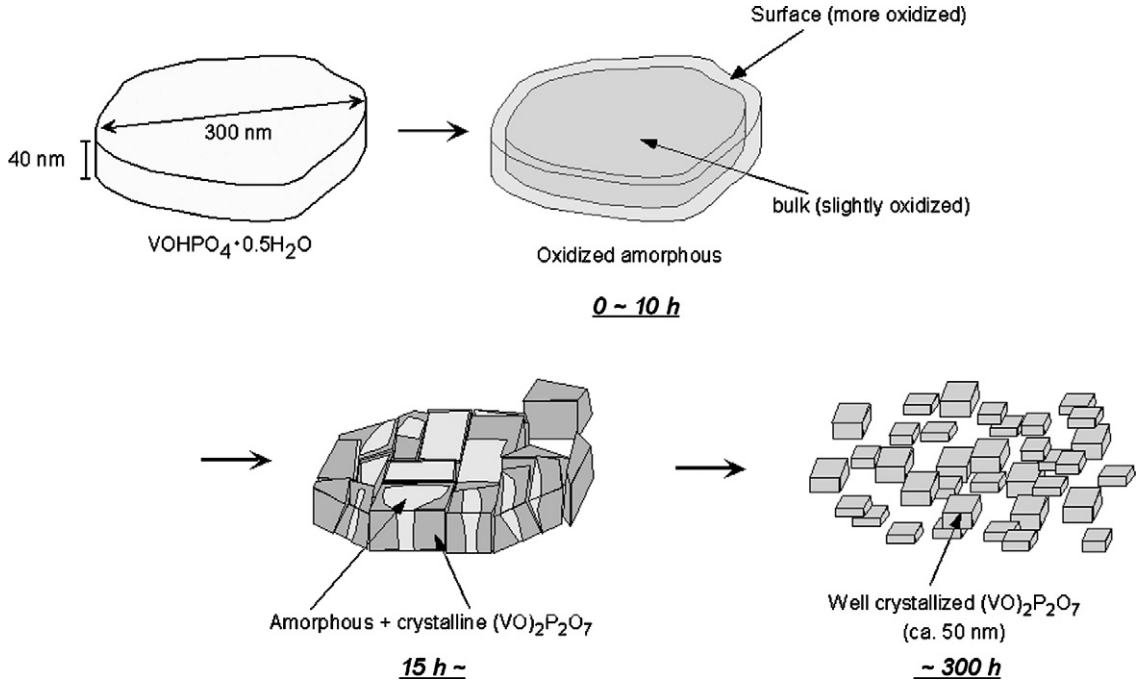

Fig. 7. Schematic models of crystallite structures during transformation from nano-sized $VOHPO_4{\cdot}0.5H_2O$ to $(VO)_2P_2O_7$.

$(VO)_2P_2O_7$ at the periphery but preventing the water inside the crystallites from escaping [9]. This promotes the formation of $VOPO_4$ phases (V^{5+}), such as δ-$VOPO_4$, inside the particle, because $VOHPO_4{\cdot}0.5H_2O$ readily transforms to δ-$VOPO_4$ under the reaction conditions [6]. In contrast, for nano-sized $VOHPO_4{\cdot}0.5H_2O$ crystallites, dehydration proceeded uniformly throughout the crystallites due to their small size, preventing the formation of oxidized $VOPO_4$ phases. Consequently, nano-sized $VOHPO_4{\cdot}0.5H_2O$ was transformed into crystalline $(VO)_2P_2O_7$ without the formation of any crystalline phases other than $(VO)_2P_2O_7$ under the reaction conditions.

As shown in Fig. 1, selectivity to MA increased rapidly during the initial 20 h and then increased more slowly with increasing treatment time. This trend closely follows the growth of crystalline $(VO)_2P_2O_7$ as confirmed by XRD (Fig. 2A) and Raman spectra (Fig. 3). Because $(VO)_2P_2O_7$ is considered indispensable for the formation of MA, although the active phases involving δ-$VOPO_4$, the X_1 phase, and the interface of V^{4+}/V^{5+} remain controversial, evolution of the $(VO)_2P_2O_7$ phase is a major reason for the increased selectivity to MA with treatment time.

In contrast to the trend in selectivity, the conversion increased to a maximum after approximately 40 h but then decreased with further treatment time. *n*-Butane is considered to be selectively activated on $(VO)_2P_2O_7$ [1–3]; thus, the increasing activity up to 40 h likely is due to formation of the $(VO)_2P_2O_7$ phase. But the decrease in activity over time cannot be explained by changes in the crystalline phases or surface area, because the formation of crystalline $(VO)_2P_2O_7$ proceeded monotonically with treatment time while the surface area continued to increase after 40 h. The selective oxidation of *n*-butane over $(VO)_2P_2O_7$ proceeds via a redox mechanism involving V^{4+} and V^{5+} at a few surface layers [20–22]. *n*-Butane is oxidized to MA over the partially oxidized phase (V^{5+}), and, consequently, the partially oxidized phase transforms to the reduced phase [V^{4+}; $(VO)_2P_2O_7$]. The reduced phase is then reoxidized by O_2 to regenerate the oxidized phase. In this mechanism, a catalyst containing a large amount of the oxidized phase should be more active. In addition, if the rate of reoxidation is slower than the rate of reduction, then the oxidation state of the surface will gradually decrease with treatment time, causing a deterioration in activity. Indeed, as shown in Figs. 5B and 6, the oxidation state of the surface decreased gradually with treatment time. The activity also decreased with a reduction in oxidation state. These results are consistent with the considerations described above.

Kamiya et al. [23] demonstrated that highly crystalline $(VO)_2P_2O_7$ has a low ratio of reoxidation to reduction rate (r_{OX}/r_{RE}); that is, the surface is difficult to reoxidize. The present catalyst system demonstrated the growth of crystalline $(VO)_2P_2O_7$ with treatment time. The growth of crystalline $(VO)_2P_2O_7$ is a likely reason for the reduction in r_{OX}/r_{RE}, which results in decreased catalytic activity with treatment time.

5. Conclusion

Nano-sized precursor $VOHPO_4{\cdot}0.5H_2O$ crystallites (300 nm long, 40 nm thick), were transformed into highly crystalline $(VO)_2P_2O_7$ through a deeply oxidized amorphous intermediate at 663 K in an *n*-butane/air mixture over 300 h. During this transformation, no crystalline phases other than $(VO)_2P_2O_7$ were formed, a result that differs significantly from the transformation in micrometer-sized $VOHPO_4{\cdot}0.5H_2O$ crystallites. The selectivity to MA increased monotonically with treatment time due to the formation of crystalline $(VO)_2P_2O_7$. In contrast, the activity increased during the early stages of transformation but then decreased over time. During the transformation, the catalyst surface oxidation state decreased gradually, causing a decrease in activity.

Acknowledgment

This work was supported by a grant from Core Research for Evolution Science and Technology (CREST) of the Japan Science and Technology Corporation (JST).

References

[1] G. Centi, F. Trifiró, J.R. Ebner, V.M. Franchetti, Chem. Rev. 88 (1988) 55.
[2] G. Centi, F. Cavani, F. Trifirò, in: Selective Oxidation by Heterogeneous Catalysis, Kluwer Academic, New York, 2001, p. 143.
[3] G.J. Hutchings, J. Mater. Chem. 14 (2004) 3385.
[4] B.K. Hodnett, Catal. Rev. Eng. 17 (1985) 373.
[5] S. Albonetti, F. Cavani, F. Trifiró, Catal. Rev. Sci. Eng. 38 (1996) 413.
[6] M. Abon, K.E. Bere, A. Tuel, P. Delochere, J. Catal. 156 (1995) 28.
[7] G.J. Hutchings, A. Desmartin-Chomel, R. Olier, J.C. Volta, Nature 368 (1994) 41.
[8] C.J. Kiely, A. Burrows, S. Sajip, G.J. Hutchings, M.T. Sananes, A. Tuel, J.C. Volta, J. Catal. 162 (1996) 31.
[9] C.J. Kiely, A. Burrows, G.J. Hutchings, K.E. Bere, J.C. Volta, A. Tuel, M. Abon, Faraday Discuss. 105 (1996) 103.
[10] L. O'Mahony, T. Curtin, J. Henry, D. Zemlyanov, M. Mihov, B.K. Hodnett, Appl. Catal. A 285 (2005) 36.
[11] M. Conte, G. Budroni, J.K. Bartley, S.H. Taylor, A.F. Carley, A. Schmidt, D.M. Murphy, F. Girgsdies, T. Ressler, R. Schlögl, G.J. Hutchings, Science 313 (2006) 1270.
[12] Y. Kamiya, N. Hiyoshi, N. Ryumon, T. Okuhara, J. Mol. Catal. A 220 (2004) 103.
[13] Y. Kamiya, N. Ryumon, H. Imai, T. Okuhara, Catal. Lett. 111 (2006) 159.
[14] H. Imai, Y. Kamiya, T. Okuhara, J. Catal. 251 (2007) 195.
[15] T. Nakato, Y. Furumi, N. Terao, T. Okuhara, J. Mater. Chem. 10 (2000) 737.
[16] N. Yamamoto, N. Hiyoshi, T. Okuhara, Chem. Mater. 14 (2002) 3882.
[17] B.K. Hodnett, P. Permannce, B. Delmon, Appl. Catal. 6 (1983) 231.
[18] G.J. Hutchings, J.K. Bartley, J.M. Webster, J.A. Lopez-Sanchez, D.J. Gilbert, C.J. Kiely, A.F. Carley, S.M. Howdle, S. Sajip, S. Caldarelli, C. Rhodes, J.C. Volta, M. Poliakoff, J. Catal. 197 (2001) 232.
[19] G.J. Hutchings, J.A. Lopez-Sanchez, J.K. Bartley, J.M. Webster, A. Burrows, C.J. Kiely, A.F. Carley, C. Rhodes, M. Hävecker, A. Knop-Gericke, R.W. Mayer, R. Schlögl, J.C. Volta, M. Poliakoff, J. Catal. 208 (2002) 197.
[20] M. Pepera, J.L. Callahan, M.J. Desmond, E.C. Milberger, P.R. Blum, N.J. Bremer, J. Am. Chem. Soc. 107 (1985) 4883.
[21] T. Okuhara, M. Misono, Catal. Today 16 (1993) 61.
[22] G. Koyano, T. Okuhara, M. Misono, J. Am. Chem. Soc. 120 (1998) 767.
[23] Y. Kamiya, E. Nishikawa, T. Okuhara, T. Hattori, Appl. Catal. A 206 (2001) 103.